Chapter 5
Production, Structure and Properties Control of Titanium Microalloyed Steel

Jixiang Gao

As a kind of microalloying element, titanium significantly improves the comprehensive properties of steel. However, when compared with niobium and vanadium microalloying technology, Ti-microalloying technology had not been extensively used in industry for a long time. It is because the properties of Ti-microalloyed steel fluctuate largely and the production process is not stable. Titanium is very active and tends to react with oxygen, nitrogen and sulfur to form large Ti-bearing phases which are harmful to the comprehensive properties of steel, such as TiO, TiS and Ti_2CS. More importantly, the formation of these phases consumes a portion of titanium. This consumption not only reduces the volume fraction of TiC precipitated at low temperatures, but also significantly changes the chemical free energy of TiC precipitation. Therefore, the precipitation behavior of TiC is remarkably changed and its strengthening effect is greatly affected. In addition, the precipitation of TiC is sensitive to temperatures and the variation of production parameters remarkably affects the properties of steel. As a result, the mechanical properties of Ti-microalloyed steel products of different batches with the same chemistry or even different locations of the same batch fluctuate greatly.

In recent years, due to the rapid development of steel production technology, the content of impurities in steel is significantly reduced and the recovery rate of titanium is effectively controlled. In addition, the research on the chemical and physical metallurgy principles of Ti-microalloyed steel promotes the development of production technology. First of all, this chapter introduces the smelting production control in the actual production process, particularly the technology of deep deoxidation, deep desulfurization and low nitrogen control. Then, the influence of the main parameters

J. Gao (✉)

Guangdong Polytechnic Normal University, Guangzhou, China
e-mail: 13602772322@163.com

of continuous casting process on the quality of Ti-microalloyed steel slabs is introduced. Finally, the effect of the parameters of hot rolling process on the microstructure and properties of Ti-microalloyed steel is elaborated.

5.1 Key Smelting Process

5.1.1 Technology of Deep Deoxidation and Inclusions Control

5.1.1.1 Deep Deoxidation Technology

Oxygen content in molten steel is one of the key indexes that evaluate the quality of molten steel. It does not only determine the amount of inclusions but also affect the size, morphology and distribution of inclusions. In order to reduce the oxygen content, aluminum, which is the strong deoxidizer, is generally used to kill the oxygen in molten steel. After deoxidation during steel tapping, the element controlling oxygen is changed from carbon to aluminum. The reaction is as follows:

$$2[Al] + 3[O] \rightarrow (Al_2O_3) \tag{5.1}$$

According to the thermodynamical data, the relationship between oxygen and aluminum in molten steel can be expressed by Eq. (5.2) [1]:

$$\lg[a_{Al}]^2[a_O]^3 = -\frac{62780}{T} + 20.17 \tag{5.2}$$

At 1600 °C, $[a_{Al}]^2[a_O]^3 = 4.5 \times 10^{-14}$.

Figure 5.1 shows the relationship between the content of aluminum and the content of dissolved oxygen according to Eq. (5.2). The content of oxygen in molten steel obviously decreases with aluminum increasing when the content of aluminum is less than 0.02%, but does not remarkably further decrease with aluminum increasing when the content of aluminum is in the range of 0.02–0.035%. And the content of oxygen keeps stable with aluminum increasing when the content of aluminum is more than 0.035%. In practice, aluminum in molten steel can easily react with oxygen in slags and also reduce SiO_2 and MnO in slags with the result of increasing the amount of aggregated Al_2O_3 in molten steel. In addition, high content of aluminum in molten steel also aggravates the re-oxidation during casting and produce Al_2O_3 inclusions.

Aluminum or aluminum-bearing deoxidizer is generally used to kill the oxygen in molten steel during tapping in the titanium microalloyed steel production process. Meanwhile, the synthetic slags with strong capabilities of deoxidation and desulphurization and lime are also used for refining slags. The content of the synthetic slag is as follows: CaO 50–55%, SiO_2 3–5%, Al_2O_3 30–35%, MgO 7–12%,

Fig. 5.1 Relationship between soluble aluminum content and soluble oxygen content in molten steel at 1600 °C
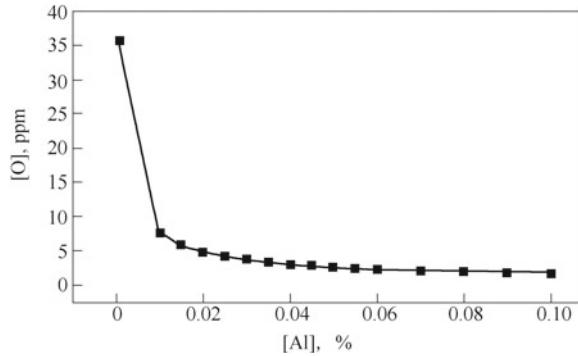
FeO + MnO < 1%. According to a large amount of production data, the matched amount of aluminum is 2–2.5 kg/t to the oxygen content in the range of 700–900 ppm.

It's very important to reserve some soluble aluminum in molten steel after deoxidization. It can be explained as follows. During the tapping process, iron and oxygen in molten steel reacts to form FeO, and manganese alloy reacts with oxygen in molten steel to form MnO. The content of FeO and MnO in refining slag in ladles is about 5% because of slagging off during tapping. The slag is black and the stability is lower than that of Al_2O_3. Thus, FeO and MnO in the slag will resolve and transfer oxygen, iron and manganese to molten steel, and aluminum in molten steel will kill the resolved oxygen further. The reaction continues until the content of FeO and MnO in the slag is less than 1%, and the slag becomes white. Finally, the oxygen in molten steel is controlled stably by aluminum.

Besides aluminum content, soft argon blowing process has a great effect on the oxygen content in molten steel. Figure 5.2 [2] shows the relationship between soft argon blowing time and content of oxygen, T[O]. T[O] decreases with the increase of argon blowing time. T[O] can be less than 15 ppm when the argon blowing time is more than 8 min, and the minimum is 10 ppm. In practice, soft argon blowing time is set to be 8–10 min in order to improve the purity of molten steel and take into account the production schedule.

5.1.1.2 Calcium Treatment Technology

Though oxygen can be controlled at low-level in aluminum killed steel, Al_2O_3 is inevitable. Al_2O_3 existing on steel plate surface can cause surface defects, and existing inside of the steel plate will deteriorate the mechanical performance. In addition, Al_2O_3 inclusions tend to gather and solidify in the inner of nozzle because the diameter of the submerged nozzle for thin slab casting is small. As a result, the nozzle is clogged, obstructing the flow of molten steel and leading to the fluctuation of liquid level. In severe case, the nozzle can be blocked and casting is interrupted. Figure 5.3 shows the morphology of a submerged nozzle and Fig. 5.4 presents the composition

of the clogs analyzed by electron probe micro-analyzer (EPMA). The inner of nozzle is covered by a thick layer of clogs, which are composed of Al_2O_3 and calcium aluminates with high melting point.

In practice, modification of Al_2O_3 by calcium treatment is usually applied to improve the surface and internal quality of steels and to prevent nozzle clogging during the continuous casting. Figure 5.5 shows the equilibrium phase diagram of $CaO–Al_2O_3$ system. The reaction is as follows.

$$x[Ca] + yAl_2O_3 = x(CaO) \cdot (y - x/3)Al_2O_3 + 2/3x[Al] \quad (5.3)$$
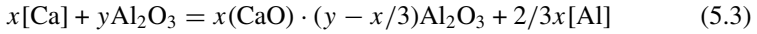
Alumina inclusions can be modified into $CaO \cdot Al_2O_3$ (CA) or $12CaO \cdot 7Al_2O_3$ ($C_{12}A_7$) according to Eq. (5.3). The melting temperature of $C_{12}A_7$ phase is 1455 °C, which is the lowest among all the phases. Therefore, $C_{12}A_7$ phase is liquid at the temperature of molten steel. $C_{12}A_7$ inclusions in molten steel tend to gather and grow up, then be removed through floating. So the purpose of calcium treatment is to modify Al_2O_3 into $C_{12}A_7$.

**Fig. 5.2** Relationship between soft argon blowing time and oxygen content in molten steel
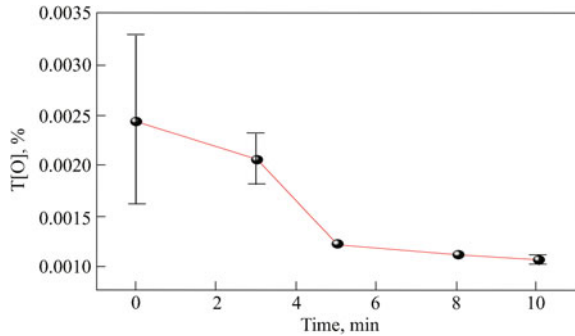
**Fig. 5.3** Submerged nozzle adhered by clogs

Figures 5.6 and 5.7 show the changes of the compositions and morphologies of inclusions before and after Ca treatment, respectively [2]. The inclusions are scraps of Al_2O_3 and $MgO \cdot Al_2O_3$ in the initial stage of refining, as shown in Figs. 5.6 and 5.7. Then Al_2O_3 and $MgO \cdot Al_2O_3$ inclusions are modified into $CaO-Al_2O_3-MgO$ inclusions during the ladle furnace (LF) refining because of the reaction between the molten steel and the refining slag with high basicity. Most inclusions are $CaO-Al_2O_3-MgO$ with high melting points before calcium treatment. The morphologies of inclusions apparently change after calcium treatment because of the reaction between calcium and Al_2O_3. The compositions of $CaO-Al_2O_3-MgO$ move to liquid region from solid region in the ternary phase diagram of $SiO_2-CaO-Al_2O_3$ (shadow region in Fig. 5.6). The inclusions have been spheroidized or are being spheroidized after calcium treatment, and most are composite inclusions. Two types of inclusions have been observed. One is the homogeneous phase of the $CaO-Al_2O_3$ system. The other is the calcium aluminates containing MgO in core and surrounded
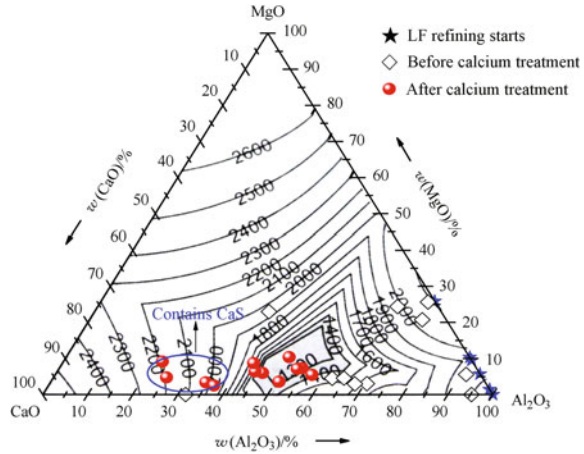
Fig. 5.4 Composition of clogs measured by EPMA
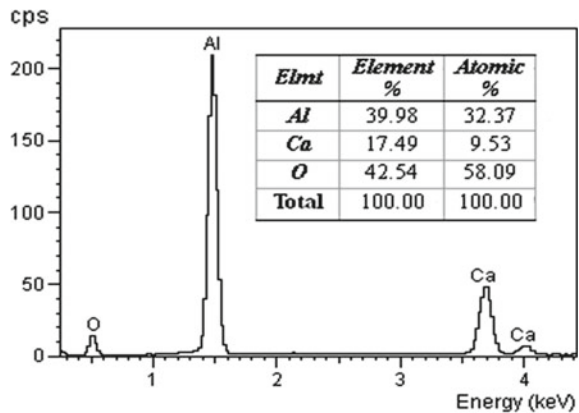
Fig. 5.5 Equilibrium phase diagram of $CaO-Al_2O_3$ system
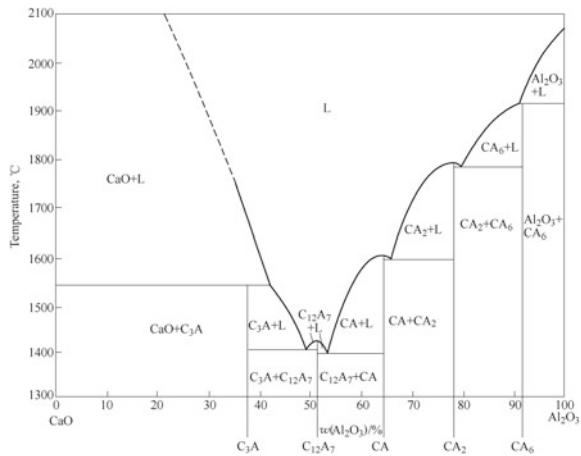
**Fig. 5.6** Changes in the composition of inclusions in molten steel during LF refining process

by CaS. The size of the later is large and they can be removed during soft argon blowing. The proportion of inclusions with the size less than 5 μm rises remarkably to more than 80% after soft argon blowing.

In practice, Al_2O_3 can be modified into $12CaO \cdot 7Al_2O_3$ or calcium aluminates with compositions close to $12CaO \cdot 7Al_2O_3$ and low melting points by calcium treatment when the ratio of calcium to aluminum is above 0.09.

5.1.2 Deep Desulfurization Technology

Desulfurization reaction can be expressed by Eq. (5.4) for titanium microalloyed steel deoxidized by aluminum [1].

$$3[S] + 2[Al] + 3(CaO) = (Al_2O_3) + 3(CaS) \tag{5.4}$$
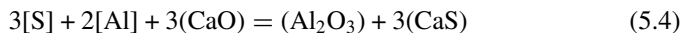
The key parameters of desulfurization during smelting are as follows.

(1) Aluminum content in molten steel. Aluminum content should be in the range of 0.04–0.05% before refining to create the conditions for rapid desulfurization. It should be in the range of 0.025–0.035% before titanium alloying after refining to improve the yield of titanium.

(2) Reducing slag for deep desulfurization. The content of Al_2O_3 in slag increases because of aluminum oxidation during desulfurization. Therefore, lime is necessary in the slag. The ratio of $w(\%CaO)/w(\%Al_2O_3)$ in slag should be about 1.8 to speed up the desulfurization reaction if the content of sulfur is high. Desulfurization can be significantly improved by the slag with high CaO content and good fluidity.
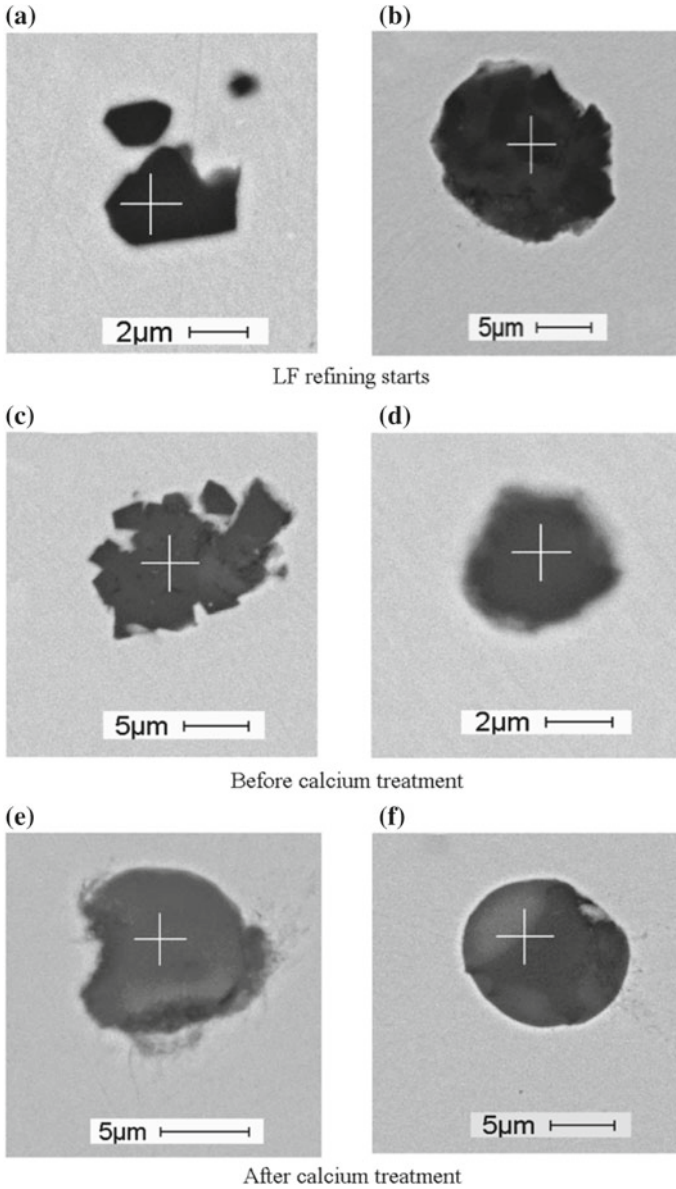
Fig. 5.7 Morphologies of the typical inclusions in molten steel during refining process

(3) Temperature. The equilibrium constant of desulfurization in Eq. (5.4) increases
     with temperature increasing, which means high temperature can promote the
     desulfurization reaction. So the temperature is generally set to be above 1600 °C.

Table 5.1 Desulfurization for titanium microalloyed high strength weathering steel

Before refining (%)	After refining (%)	Average desulphurization rate (%)	Max rate (%)	Min rate (%)
0.0193	0.004	79.27	92.59	75.2

(4) Argon blowing process. The argon pressure should be more than 0.75 MPa during refining to promote desulfurization reaction.

Table 5.1 shows the desulfurization for titanium microalloyed high strength weathering steel. The desulphurization rate during refining is 75.2–92.59% by the methods above, the average rate is 79.27%, and the sulfur content is less than 40 ppm at the end of refining.

### 5.1.3 Low Nitrogen Steelmaking Technology

Coarse TiN tends to precipitate in molten steel by the reaction between nitrogen and titanium when the content of nitrogen is high. And as a consequence, the beneficial effect of titanium is reduced. Therefore, nitrogen content should be strict controlled in titanium microalloyed steel.

Pillild investigated the change of nitrogen content in the smelting process by electrical arc furnace (EAF), as shown in Fig. 5.8 [3]. Symbol A presents the period of electrode insertion, during which the nitrogen content keeps stable. Symbol B presents the first charge and the formation of small molten bath. Because the surface area of scraps during smelting is large and there is no slag covered on molten steel, the nitrogen content increases obviously by absorbing nitrogen from the electrode zone. Symbol C presents the development of molten bath. In the period, the amount of molten steel in molten bath and volume of slag increase, while the amount of nitrogen picking up reduces. So the nitrogen content decreases because of the dilution by increasing melting steel. Symbol D presents the period of scrap melting down and heating to the temperature for carbon-oxygen reaction. The nitrogen content remains unchanged because there is no denitrification. Symbol E presents the period of decarburization. And much nitrogen is removed by carbon-oxygen reaction. Symbol F presents the period of shielding arc heating to tapping temperature. The nitrogen content doesn't change because of the terminal reaction between carbon and oxygen. Symbol G presents the period of tapping. Nitrogen content increases because of the nitrogen picking up from air. Symbol H presents the period of steel holding in ladle, during which the nitrogen content keeps unchanged. Then, the nitrogen content increases a little during casting (symbol I).

The nitrogen in scraps has a significant influence on the nitrogen content in molten steel after scrap melting down, as shown in Fig. 5.9 [4]. So proper charging is very important to reduce the nitrogen content introduced by scraps.

Fig. 5.8 Change in nitrogen content during EAF smelting process
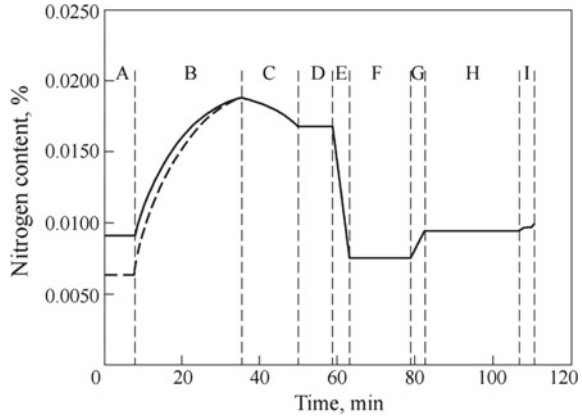
Due to more amounts of microalloying elements added and the nitrogen solubility increased by microalloying elements, denitrification for titanium microalloyed steel is even more difficult. Therefore, the key of nitrogen controlling for titanium microalloyed steel is to reduce nitrogen picking up in each process. The methods are as follows:

(1) Remove the nitrogen in converter during steelmaking. The nitrogen is mainly removed in converter because of the good kinetics conditions. The technologies for low nitrogen steelmaking are presented as follows.

   (1) Technology of controlling bottom blowing process in converter. Types and flow rate of bottom blowing gas influence the nitrogen content in molten steel at the end of steelmaking. The switch from nitrogen to argon is usually carried out during the intermediate stage of blowing, and the intensity

Fig. 5.9 Influence of nitrogen content in steel scraps on nitrogen content after scraps melting down
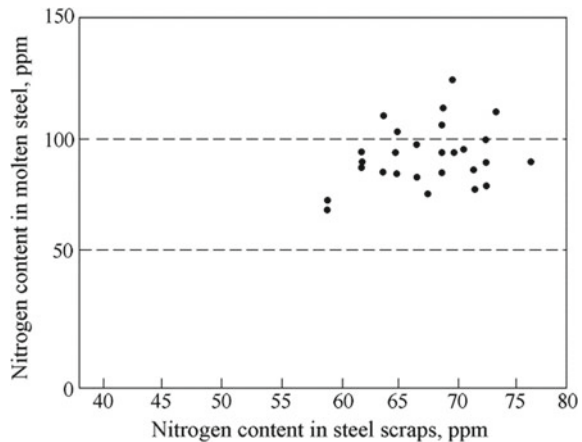
of bottom blowing gas increases gradually. The intensity of argon keeps maximum during the intermediate and the final stage of blowing. And the argon blowing time is more than 1 min before tapping. In addition, inspection and maintenance on the bottom blowing system are necessary to ensure the effect of blowing for all purging plugs.

(2) Technology of end-point carbon and temperature controlling in converter. The end-point carbon and temperature influence the operation of LF refining, such as deoxidization, temperature controlling and so on. Therefore, it is in favor of the nitrogen controlling in LF refining to have the reasonable end-point carbon and temperature.

The molten steel tends to pick up nitrogen from air during the contacting because of the high content of nitrogen in air. The methods to reduce nitrogen picking up in practice are shown as follows. Clean up the slag remained outside of the tap hole before steelmaking. Change the tap hole in the case of long tapping time or bad slag damming. Maintain the tap hole and reasonably control the tapping time. Blow argon to the ladle before tapping to reduce the nitrogen pickup. Cover the surface of molten steel with synthetic slag to insulate molten steel from air, by which to reduce the nitrogen pickup during tapping. The nitrogen content is less than 25 ppm after tapping by the methods above.

During EAF steelmaking, nitrogen pickup of molten steel is mainly from the nitrogen in scraps, the ionized nitrogen in the arc zone and the absorbed nitrogen from air during tapping. Accordingly, the methods to reduce nitrogen pickup are presented as follows. Charge reasonably to reduce the nitrogen introduced by scraps. Foam slag during EAF steelmaking to prevent the exposure of molten steel to the open air and nitrogen absorption. In addition, cover the surface of molten steel with synthetic slag to insulate molten steel from air, by which to reduce the nitrogen pickup during tapping.

Nitrogen can be removed by the large amount of CO bubbles produced during the decarburization of EAF steelmaking process because of the strong stirring effect of CO bubbles on the molten steel. The amount of denitrification increases with the amount of decarburization or the CO bubbles produced during decarburization. In order to ensure the high capacity of denitrification during EAF steelmaking, charging with high carbon (by addition of pig iron and HBI) and increasing the oxygen blowing intensity are necessary.

(2) Reduce nitrogen pickup during LF refining. Prevention of nitrogen pickup is the main measure during LF fining because LF furnace doesn't have the function of denitrification. The introduced nitrogen from scraps and the absorbed nitrogen from air are the main causes of nitrogen pickup during LF refining. Accordingly, the methods to reduce nitrogen pickup are presented as follows. Charge reasonably to reduce the nitrogen introduced from scraps. Heat the molten steel rapidly to the target temperature by the technology of slagging with short-arc and submerged-arc, which can reduce the heating time and prevent nitrogen absorption. In addition, controlling the stirring intensity during

refining and maintaining the vapor pressure over air pressure are also important to reduce nitrogen absorption. The nitrogen pickup can be controlled to be less than 5–10 ppm by the methods above.

(3) Reduce nitrogen pickup during continuous casting. The exposure of molten steel to air is the main source of nitrogen pickup during casting. Therefore, casting with whole-process protection is adopted to reduce or prevent reoxidation of molten steel. For example, ladle covering flux is put on the surface of molten steel after refining to prevent reoxidation. Ladle with the heat insulating cover is used to reduce the temperature drop. Long nozzle casting with shielding argon is also used to prevent reoxidation of molten steel by air. Tundish covering flux is put on the surface of molten steel to prevent reoxidation. According the methods above, the nitrogen content of molten steel by converter steelmaking is about 40 ppm, while it's about 60 ppm by EAF steelmaking.

5.1.4 Control of the Yield of Titanium

Because Ti is very active, Ti is prone to react with oxygen, nitrogen and sulfur in molten steel, leading to the low and unstable yield of titanium. Therefore, increasing and stabilizing the yield of Ti is the key during steelmaking for Ti microalloyed steel. The technologies of deep deoxidization, desulphurization and low nitrogen steelmaking are developed and applied in practice, which can keep the contents of oxygen, sulfur and nitrogen at low levels. Meanwhile, the appropriate addition process for Fe–Ti alloy should be developed. The addition of Fe–Ti alloy should be prior to the end of refining. The molten steel should be well deoxidized, of which the oxygen content is less than 0.003% and the aluminum content is in the range of 0.025–0.035%. It is beneficial to raising and stabilizing the yield of titanium [5]. Table 5.2 shows the industrial test data by the methods above. The yield of Ti during refining is 70–80% for the molten steel by EAF steelmaking, while it is 75–85% by converter steelmaking because of the lower nitrogen content.

5.2 Key Technologies for Continuous Casting

5.2.1 Key Process Parameters

In order to ensure the Production of continuous casting, no steel leaking and slab quality for titanium microalloyed steel, the casting process should be designed by the following principals besides the composition, cleanliness and inclusion morphology of molten steel. Increase the cooling rate of ingot as much as possible to refine the precipitates. Protect the whole casting process to reduce and prevent re-oxidation of molten steel. Solve the problems relevant to casting temperature, settings of the vibra-

Table 5.2 Yield of titanium for titanium microalloyed steel by EAF steelmaking

No.	Weight of molten steel (t)	Amount of Ti–Fe (kg)	Residual Ti (%)	Ti at the end of refining (%)	Yield of Ti (%)
104044760	151.1	170	0.002	0.0375	78.9
104063890	152.7	270	0.001	0.056	79.2
104080770	151.2	330	0	0.063	72.2
204113760	154	350	0.001	0.069	74.8
204113770	155	360	0	0.065	70.0
205031770	155		0.001	0.088	74.9
205031780	152.5	670	0	0.126	71.7
205031790	155	700	0	0.133	73.6
Average	153.8				73.9

tion curves and setting of the secondary cooling system. Optimize the mould flux, and match the speed and the temperature. Increase the charging temperature of ingot. The methods all above can improve the surface and internal quality of slabs.

(1) Casting temperature system. The reasonable casting temperature system is very important to the casting process and the improvement of the slab quality. High casting temperatures will aggravate the center segregation and the thickness inhomogeneity of the initially solidified shell at the meniscus of mould, leading to the thinning of the shell leaving mould and slab cracks and even breakout. Low casting temperatures will decrease the fluidity of molten steel and influence the smelting of mould flux, which will lead to longitudinal cracks. The liquidus temperature of titanium microalloyed steel is 1523–1524 °C when the content of titanium is in the range of 0.038–0.14%. The production data show that it can prevent the breakout and improve the slab quality by controlling the superheat in the range of 20–30 °C.

(2) Protecting the whole casting process. In order to prevent the re-oxidation of molten steel and improve the slab quality, the casting process is protected in the whole process. The methods include protection for molten steel in ladles, long nozzle casting with shielding argon gas, protection for molten steel in tundish and application of submerged nozzle. Tundish covering fluxes are put on the surface of molten steel to prevent re-oxidation.

(3) Optimizing the mould flux. A few issues need to be taken into account for selecting the mould flux, such as the matching of the melting point of mould flux to the liquidus temperature of steel, the matching of the melting rate (or powder consumption) of mould flux to the casting speed, the matching of the bulk density and moisture content of mould flux to the superheat of molten steel, the matching of the basicity and viscosity of mould flux to the Ti content of molten steel and so on. The surface quality of slabs is acceptable and can meet the requirements of the industrial use only when the properties of mould flux are stable and match with the casting speed and superheat.
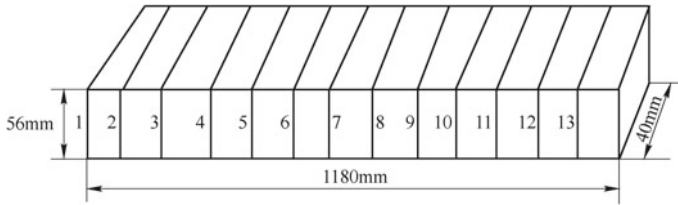
Fig. 5.10 Schematic diagram of sampling from the cast slab

(4) Controlling the casting speed. The casting speed should not only take into account the matching of the cracking sensitivity of steel to the temperature of molten steel, but also the connection between each process. In practice, the casting speed is usually limited by the processing time during refining for sequential continuous casting.

(5) Choosing the oscillation types of caster mould. Different oscillation types are chosen during the casting process for titanium microalloyed steel, which is significantly important to the surface quality of slabs and the casting process without breakout and sticking. The oscillation type is sinusoidal oscillation for thin slab casting. The amplitude increases with the casting speed and the negative strip rate is about 21%. Generally, the amplitude varies for different casters.

(6) Controlling the heat flux density in the mould. The heat flux density in the mould and the ratio of the heat flux on the narrow side to the wide side are the very important casting parameters, which can reflect the thickness of initially solidified shell. They are significant for estimating the change of the properties of mould flux, the quality of molten steel and the condition of casting. Maintaining the stable and suitable ratio of heat flux on the narrow side to the wide side can improve the slab quality. In addition, it is effective to improve the slab quality on the narrow side (e.g. cracks by hot-shortness) by adjusting the mould taper and maintaining the suitable cooling intensity.

5.2.2 Control of Slab Quality

5.2.2.1 Analysis of Slab Quality

Analysis of Composition Segregation of Slab [6]

The segregations of carbon, silicon, manganese, phosphorus, sulfur and titanium in the cross section of slab of titanium microalloyed steel produced by thin slab casting and direct rolling (TSCR) are investigated by in situ metal analyzer. The composition is 0.05%C–0.45%Si–0.45%Mn–0.08%P–0.005%S–0.07%Ti. Figure 5.10 shows the schematic of sampling. The widths of No. 1 and No. 13 are 95 mm, and the widths of No. 2 to No. 13 are 90 mm.

Figure 5.11 shows the two dimensional contour maps for each element in the cross section of slab by stitching together the two-dimensional contour maps for each element of the 13 samples. The segregation band caused by carbon segregation is obvious in the center of slab and it's the most severe segregation. Segregation bands caused by phosphorous and sulfur are also observed in the center of slab, but the segregations are less severe than that of carbon. The segregations of silicon, manganese and titanium are not distinct and there are no significant segregation bands in the center of slab.

Analysis of Slab Density

The distribution of density in the cross section of slab is shown in Fig. 5.12. The density is high and within the range of 0.924–0.955. Little difference is observed among the densities of all samples. In addition, there is no sharp reduction of density in the center of the cross section of slab. The result of in situ analysis shows that there are no central porosity and line shrinkage.

Analysis of Inclusions

Figure 5.13 shows the distribution of the content of alumina inclusions in the samples. The distribution of inclusions is homogeneous in the cross section of slab, and the content of inclusions fluctuates in the range of 0.0014–0.0022%. The results are consistent with the characteristics of inclusions exiting in slab and the content fluctuation is within the normal range.

5.2.2.2   Effect of Liquid Core Reduction on Slab Quality [7]

Liquid core reduction refers to the following process. Press the solidified shell in the mould exit and keep the liquid core in the slab, then the liquid core keeps shrinking until it completely solidifies by passing the segments of secondary cooling. In practice, liquid core reduction affects the quality of slab. This section will introduce the effect of liquid core reduction on the composition segregation and density of slab.

The slab with the thickness of 60 mm is pressed until the thickness is reduced to 55 mm by liquid core reduction equipment. The sample with liquid core reduction is labeled No. 1. Meanwhile, the sample without liquid core reduction on the same slab is labeled No. 2. The segregations of the elements and densities of the cross sections of the two samples are measured by in situ metal analyzer. Figure 5.14 shows the schematic diagram for sampling at 1/2, 1/4 and the right edge locations along the width of slab. The samples from the three different locations on No. 1 slab are labeled No. 11, No. 12 and No. 13 respectively. And the reference samples from No. 2 slab are labeled No. 21, No. 22 and No. 23 respectively.

Effect of Reduction on Segregation of Slab

Table 5.3 shows the effect of reduction on the segregation of slab. The segregation of carbon in the center of slab is obviously alleviated by liquid core reduction, and less
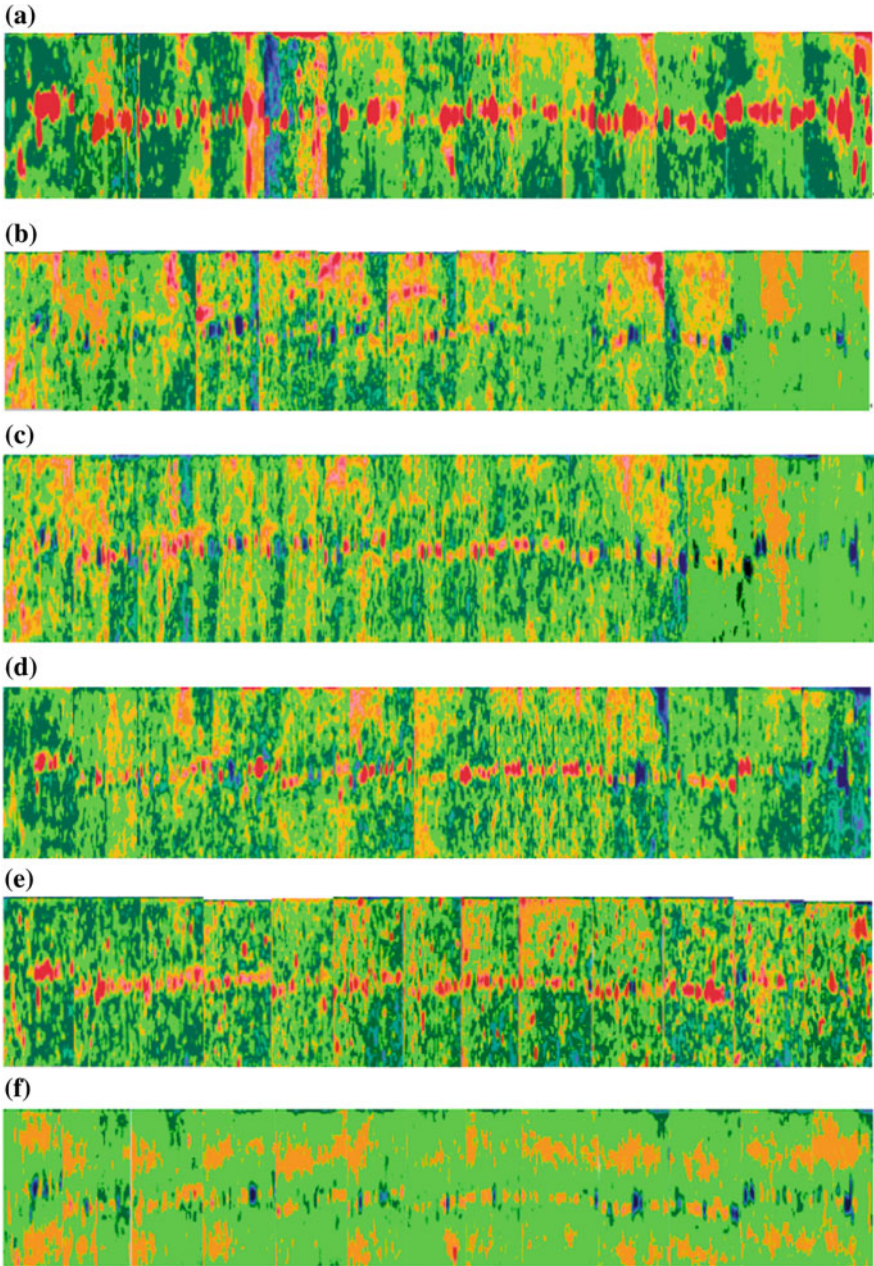
Fig. 5.11 Two dimensional contour maps for the elements in the cross section of the cast slab **a** Carbon, **b** Silicon, **c** Manganese, **d** Phosphorous, **e** Sulfur, **f** Titanium
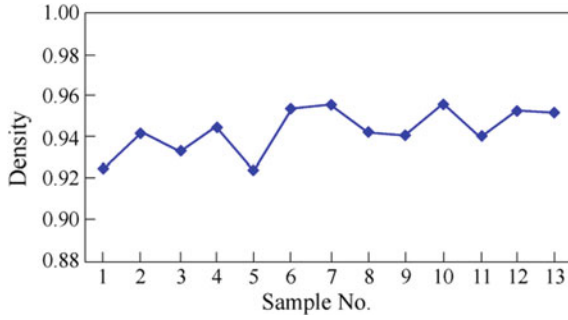
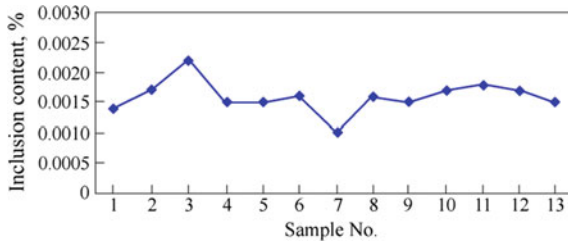**Fig. 5.12** Distribution of density across the cross section of the cast slab

Fig. 5.13 Distribution of alumina inclusion content across the cross section of the cast slab
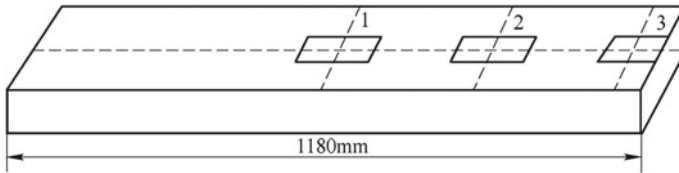

Fig. 5.14 Schematic diagram of sampling from the cast slab

obviously improved at 1/4 location along the width of slab. However, the segregation aggravates at the edge of slab. The segregations of other elements are improved, but not significantly.

Analysis of Slab Density

Figure 5.15 shows the densities of different locations of slabs with and without liquid core reduction. The result shows that the density of slab is remarkably improved by liquid core reduction.

Table 5.3 Effect of liquid core reduction on the segregation of slab

Items		With liquid core reduction			Without liquid core reduction		
		No. 11	No. 12	No. 13	No. 21	No. 22	No. 23
C	Average content (%)	0.040	0.040	0.039	0.038	0.039	0.039
	Maximum segregation	4.405	1.943	11.856	29.42	3.893	3.546
Si	Average content (%)	0.428	0.428	0.423	0.434	0.433	0.435
	Maximum segregation	1.137	1.068	1.155	1.114	1.119	1.180
Mn	Average content (%)	0.434	0.436	0.432	0.431	0.430	0.429
	Maximum segregation	1.067	1.078	1.117	1.045	1.150	1.152
P	Average content (%)	0.077	0.079	0.078	0.081	0.080	0.080
	Maximum segregation	1.342	1.219	1.235	1.391	1.349	1.478
S	Average content (%)	0.007	0.007	0.007	0.008	0.008	0.008
	Maximum segregation	1.992	1.345	2.195	1.503	1.443	1.908
Ti	Average content (%)	0.063	0.064	0.066	0.066	0.064	0.064
	Maximum segregation	1.157	1.123	1.087	1.262	1.199	1.382
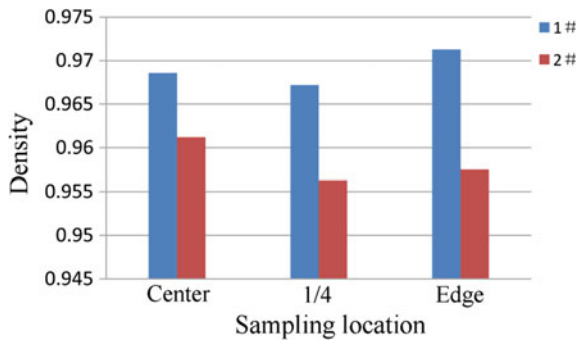
Fig. 5.15 Comparison of densities of the cast slabs with and without liquid core reduction

5.3 Key Hot Rolling Processes

The size, morphology and volume fraction of precipitates are important factors to determine the strengthening effect of Ti-microalloyed steel. The temperature and reduction schedules of hot rolling process affect the precipitation behavior of titanium, and thus have an important effect on the microstructure and properties of

final products. According to the precipitation behavior of Ti(C, N), it is important to develop a reasonable hot rolling schedule so as to improve the overall properties of Ti-microalloyed steel.

5.3.1 Temperature Schedule

Temperature is one of the most important factors affecting the precipitation behavior of Ti(C, N). The temperature schedule of hot rolling process mainly includes the discharge temperature, the finishing temperature and the coiling temperature.

5.3.1.1 Discharge Temperature

The discharge temperature of TSCR process is generally in the range of 1100–1200 °C. According to the thermodynamic condition, TiN precipitates in this temperature range. TiN precipitates have been observed by scanning electron microscopy (SEM), but the difference among the precipitates precipitated at different temperatures is not obvious. In order to further analyze the effect of discharge temperature on the properties of Ti-microalloyed steel, a large number of production data are analyzed statistically. The results are shown in Figs. 5.16 and 5.17.

According to the results, there is no evident regularity to describe the effect of discharge temperature on the mechanical properties of Ti-microalloyed steel. Low discharge temperature should be applied, which has two benefits. One is to reduce the growth and coarsening tendency of TiN precipitates during the reheating process. The other is to minimize the precipitation of TiN at high temperatures which leads to
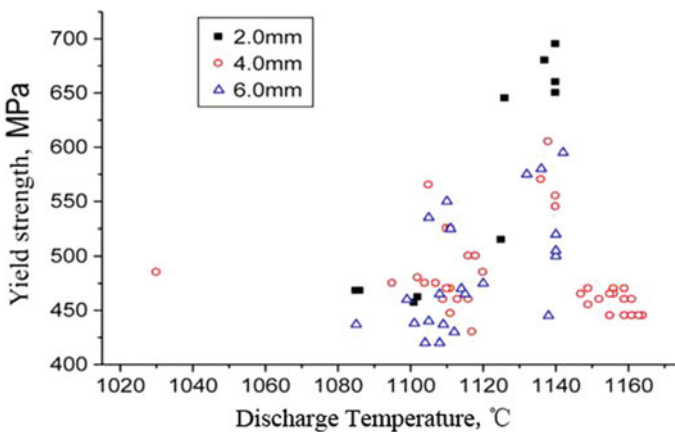

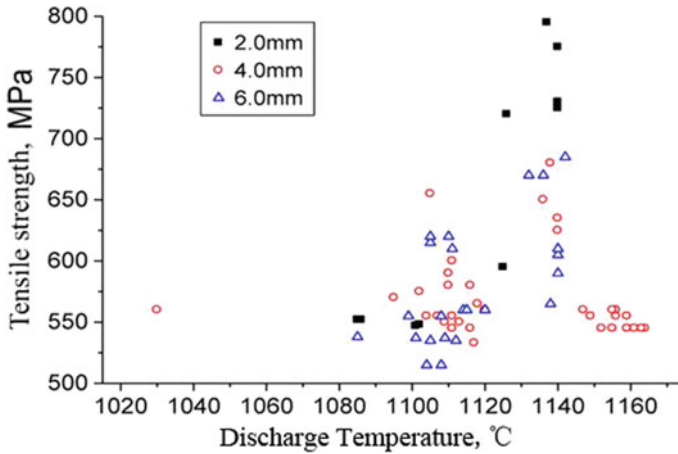Fig. 5.16 Relationship between discharge temperature and yield strength

Fig. 5.17 Relationship between discharge temperature and tensile strength

precipitation of more fine TiN precipitates at lower temperatures. Taking into account the load capacity and rolling stability of current mills, the discharge temperature is selected to be above 1120 °C.

5.3.1.2 Finishing Temperature

The effect of finishing temperature on the properties of Ti-microalloyed steel is complicated. Low finishing temperature refines ferrite grains, thereby improving the grain refinement strengthening. However, low finishing temperature induces the deformation induced precipitation of carbonitrides. These carbonitride precipitates inhibit the growth of austenite grains and contribute to a certain effect of grain refinement strengthening and precipitation strengthening. However, they are relatively large compared to the nano-scale particles precipitated in ferrite, reducing the precipitation strengthening effect. Therefore, high finishing temperature suppresses the deformation induced precipitation of Ti(C, N) in high temperature austenite and thus promotes the dispersive precipitation of TiC in ferrite, which improves the precipitation strengthening effect. But high finishing temperature is not advantageous to refinement of ferrite grains, and reduces the grain refinement strengthening effect to some extent. Figures 5.18 and 5.19 show the statistical results of production data. Different from plain carbon steel, decrease in the finishing temperature cannot improve the strength of Ti-microalloyed steel, on the contrary, if the finishing temperature increases from 860–880 °C to 890–900 °C, the strength is significantly improved.
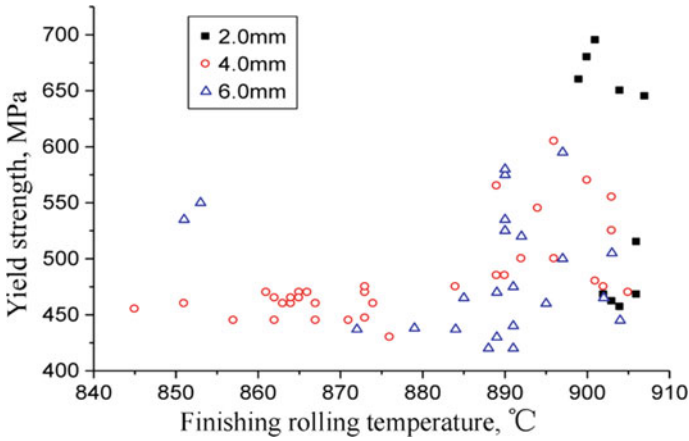
Fig. 5.18 Relationship between finishing temperature and yield strength
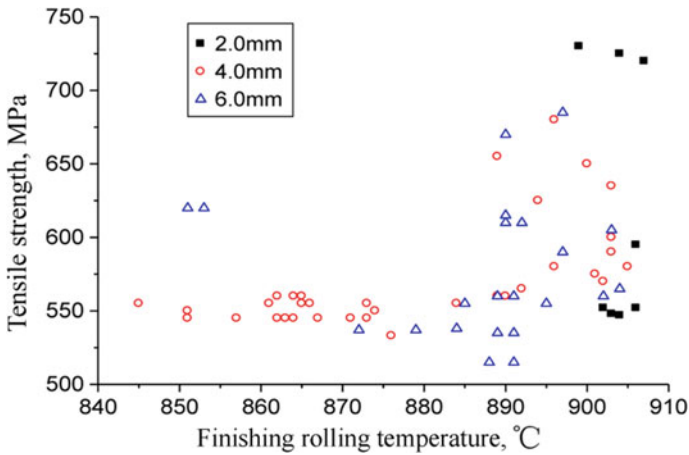
Fig. 5.19 Relationship between finishing temperature and tensile strength

5.3.1.3 Coiling Temperature

The coiling temperature is a key factor affecting the precipitation behavior of precipitates of Ti-microalloyed steel. Production data shown in Figs. 5.20 and 5.21 indicate that the coiling temperature has a significant impact on the strength of steel. The strength reaches the maximum when the coiling temperature is in the range of 580–610 °C.
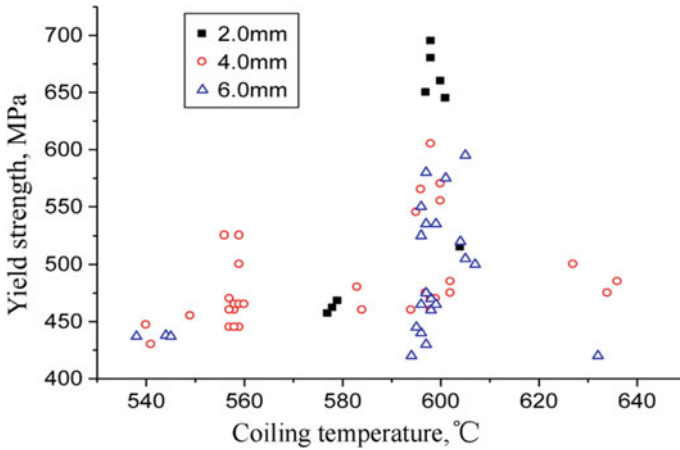
Fig. 5.20 Relationship between coiling temperature and yield strength
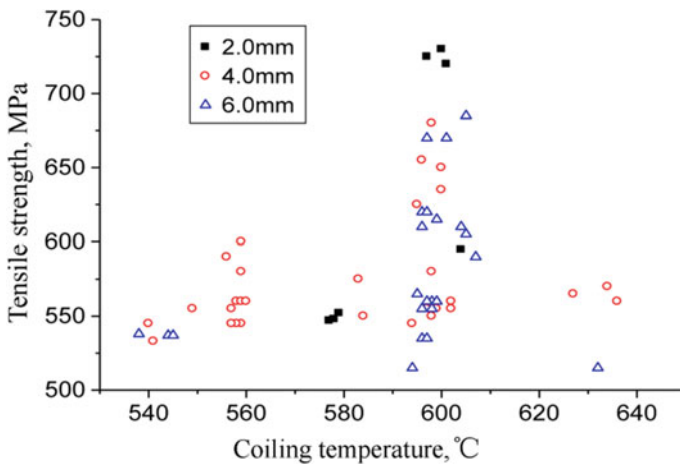
Fig. 5.21 Relationship between coiling temperature and tensile strength

5.3.2 Reduction Schedule and Reduction Ratio

The results of the comparison tests using different reduction schedules are shown in Table 5.4. The slabs are from the same batch. The effect of reduction schedules on the strength is not evident according to the results. In the production process, F1 and F2 stands should apply large reduction ratio of more than 50% as much as possible so as to avoid the occurrence of mixed grains.

Table 5.4 Production data showing the relationship between reduction schedule and strength

Heat No.	Coil No.	Ti content in production (%)	Thickness (mm)	Reduction rate (%)						Yield strength (MPa)	Tensile strength (MPa)
				F1	F2	F3	F4	F5	F6		
1	1	0.062	6.0	41.58	44.23	31.85	25.65	21.23	14.62	470	560
	2	0.062	6.0	55.39	53.03	0	34.18	0	19.48	465	560
	3	0.062	6.0	52.78	56.46	0	32.58	0	20.04	465	555
	4	0.060	6.0	52.78	56.22	0	32.72	0	20.32	475	560
	5	0.063	6.0	53.20	56.39	0	32.06	0	20.06	525	610
2	1	0.068	6.0	41.60	43.37	31.87	25.67	21.24	15.81	535	615
	2	0.068	6.0	48.57	47.60	34.97	0	23.31	17.35	550	620
	3	0.068	6.0	48.05	48.20	35.14	0	23.16	17.33	535	620

In addition, the reduction ratio is one of the main factors affecting the strength. As shown in Figs. 5.22 and 5.23, suppose equal thickness of the initial cast slabs, the thinner the product gauge, i.e. the greater the reduction ratio, the finer the grains of the product.

5.4   Comprehensive Controlling Technology for Microstructure and Properties
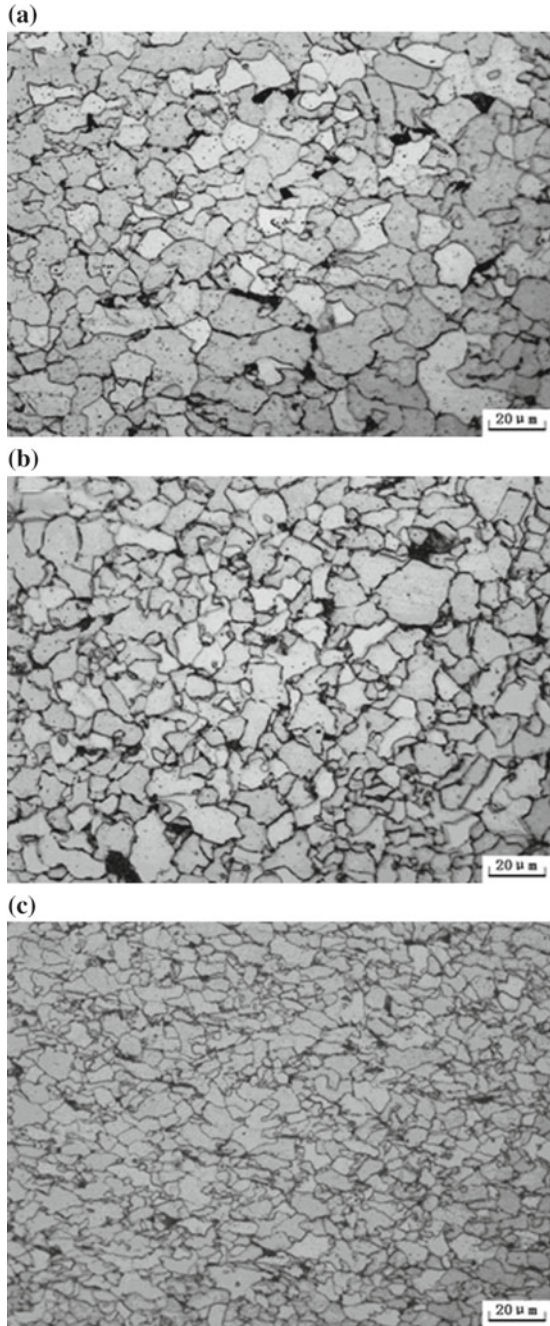
5.4.1   Effect of Titanium Content on Yield Strength

Figure 5.24 shows the relationship between yield strength and titanium content. The effect of titanium content on the strength of steel is divided into three regions. When the titanium content is lower than 0.045%, the yield strength increases slowly with the titanium content. When the titanium content is between 0.045 and 0.095%, the yield strength increases linearly with the titanium content. When the titanium content is more than 0.095%, the yield strength remains basically unchanged. The increase in the titanium content significantly improves the yield strength, and the yield strength can reach 750 MPa and more [8].

5.4.2   Controlled Rolling Patterns of Ti-Microalloyed Steel

There are two methods to refine the grains of microalloyed steel produced by controlled rolling. One is recrystallization controlled rolling and the other is non-recrystallization controlled rolling. The former method refines austenite grains by repeated recrystallization of austenite in the hot rolling process, and ultimately refines ferrite grains. The effect of microalloying elements is to control the coarsening of recrystallized austenite grains during rolling and after rolling. Representative steel are V–N and V–Ti–N microalloyed steel. For the non-recrystallization controlled rolling, austenite does not experience recrystallization during the whole process or the last several passes of finishing rolling, and transforms into pan-caked austenite with a high density of defects. Therefore, the nucleation rate of ferrite is improved and thus the final ferrite grains are refined. Almost all steel produced by non-recrystallization controlled rolling contain niobium, because niobium has a strong inhibitory effect on the austenite recrystallization. The inhibitory effect of titanium on recrystallization is between that of niobium and vanadium. The coarse microstructure of original austenite in Ti-microalloyed steel produced by TSCR can achieve complete static recrystallization through a significant high temperature deformation exerted by F1 stand. TiN particles precipitated in cast slabs effectively prevent the coarsening of recrystallized austenite grains, realizing the recrystallization controlled rolling. The dragging effect of titanium solute and the strain-induced precipitates of TiC inhibit
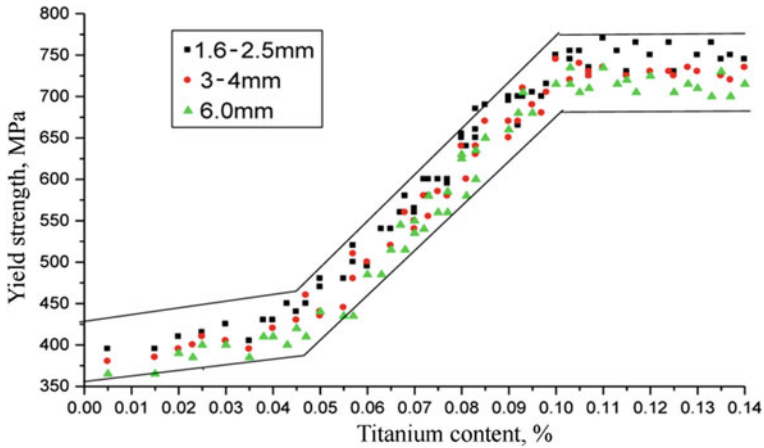
Fig. 5.22 Microstructure of
titanium microalloyed steel
plates with different
thicknesses: **a** 6.0 mm, **b**
4.0 mm, **c** 1.6 mm
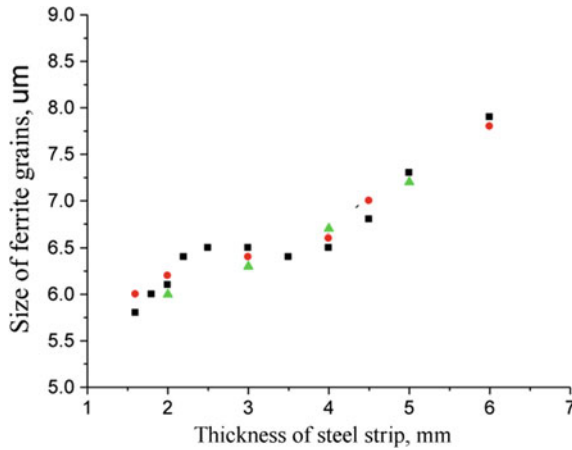
Fig. 5.23 Relationship between the size of ferrite grains and the thickness of titanium microalloyed steel (0.0558% Ti)

Fig. 5.24 Relationship between yield strength and titanium content

the recrystallization of austenite to some extent, realizing the non-recrystallization controlled rolling. By effectively controlling the parameters of hot rolling process, this joint controlled rolling pattern of recrystallization controlled rolling and non-recrystallization controlled rolling for producing Ti-microalloyed steel can be realized in the TSCR process [9].

5.4.3 Strengthening Mechanism of Ti-Microalloyed High Strength Steel

The main strengthening mechanisms of steel shown in Fig. 5.25 include solute strengthening, dislocation strengthening, grain refinement strengthening and precipitation strengthening.

The yield strength of steel can be described according to the extended Hall-Petch formula:

$$\sigma_y = \sigma_i + \sigma_{ss} + \sigma_p + \sigma_d + \sigma_{gs} \tag{5.5}$$

where σ_i is the internal lattice strengthening, $\sigma_i = 48$ MPa for low carbon steel
σ_{ss} is the solute strengthening
σ_p is the precipitation strengthening
σ_d is the dislocation strengthening
σ_{gs} is the grain refinement strengthening, $\sigma_{gs} = Kd^{-1/2}$.

Solute Strengthening The main microscopic mechanism of solute strengthening is the elastic interaction. The entrance of solute atoms into the crystal lattice of matrix distorts the lattice. The distortion produces elastic stress fields, which interact with the elastic stress fields around the dislocation. The solute strengthening effect is related to the amount of solute atoms. It is generally regarded that the solute strengthening effect in a certain composition range is proportional to the amount of solute. The proportional coefficient, i.e. the yield strength increment k_M produced by 1 mass
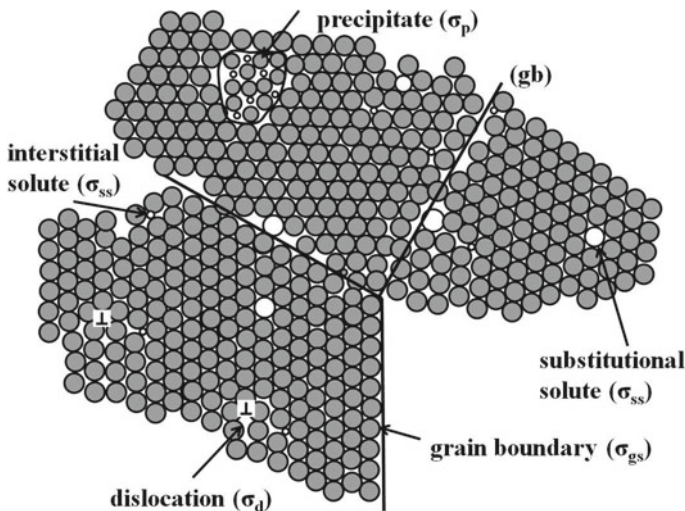

Fig. 5.25 Main strengthening mechanisms of steel

percent of solute, can be measured by experiments. Yong et al. [10] summarized the commonly used strengthening coefficients, as shown in Table 5.5.

The amount of element dissolved in steel is equal to the element content of steel if the element exists only in the form of solute in steel. For the element that exists either as solute in steel or in secondary phase, the respective amount of element dissolved in steel and in secondary phase must be theoretically calculated or experimentally measured based on the thermal history and equilibrium solubility at different temperatures. The solute strengthening increment is only related to the amount of element dissolved in steel [M].

A large number of experiments have confirmed that the increase in the yield strength of general dilute solid solution due to solute strengthening can be expressed by Eq. (5.6).

$$\Delta\sigma_s = 37[Mn] + 83[Si] + 59[Al] + 38[Cu] + 11[Mo] + 33[Ni] - 30[Cr]$$
$$+ 680[P] + 2918[N] \tag{5.6}$$

where [M] is the mass percent of solute.

Nitrogen is mainly fixed by titanium in the form of TiN in Ti-microalloyed steel. Even in the case of low titanium content, nitrogen is fixed by aluminum to form AlN. Therefore, the content of nitrogen dissolved in steel is very low and can be ignored. Titanium in steel mainly combines with carbon, nitrogen and sulfur to form a variety of compounds so the content of titanium dissolved in steel is also very low and can be ignored. A part of carbon combines with titanium to form Ti(C, N) and another part forms cementite Fe_3C. However, there is still a considerable amount of carbon dissolved in ferrite so the strengthening effect should be taken into account. According to the chemical phase analysis of Ti-microalloyed steel, the content of carbon dissolved in ferrite [C] is taken as 0.01 wt%. Elements, such as manganese, copper, silicon, phosphorus, chromium and nickel, are present in steel in the form of solute, and their amounts dissolved in steel are directly obtained from the steel composition. The calculated solute strengthening increment is 120–140 MPa.

Dislocation strengthening Dislocation strengthening is one of the effective methods to strengthen metal materials. The relationship between flow stress and dislocation density ρ is described by the following equation:

$$\sigma_d = M\alpha\mu b\rho^{1/2} \tag{5.7}$$

where M is the orientation factor and α is the proportional coefficient.

Dislocation density mainly depends on the reduction ratio. In general, the larger the reduction ratio and the lower the finishing temperature there are, the higher the dislocation density and the greater the dislocation strengthening contribution to the yield strength there will be. σ_d is very small and does not exceed 45 MPa in the temperature range of the formation of polygonal ferrite. The dislocation density in ZJ330B steel sheet with a thickness of 1.0 mm is 2.8×10^{13} m/m^3, and the calculated dislocation strengthening contribution to the yield strength is 46.1 MPa [11]. The dislocation strengthening contribution is different among Ti-microalloyed high

Table 5.5 Yield strength increment k_M produced by 1 mass percent of solute in ferrite (MPa)

C (solubility < 0.2%)	N (solubility < 0.2%)	P	Si	Ti	Cu	Mn	Mo	V	Cr	Ni	Sn	Comment
		247	82		96	70	8			33	113	
	354.2		83			32						
	2918		83			37						
		677	59			40						
			84			33						
4370	3750	350	86		39	50	22					
4570	4570	67.6	84	80	38	32	11	3	−30	0		
		468										
5000	5000	680	84		38	32	11		−30	33		
	5197											
4570	4570	470	83	80	38	37	11	3	−30	0	113	Recommended Value

strength steel sheets with different gauges. The lower the finishing temperature and the thinner the sheets, the greater the strengthening effect. The dislocation strengthening contribution is taken as 20–40 MPa for Ti-microalloyed high strength steel sheets with different gauges.

Grain refinement strengthening Researchers are always devoted to research on grain refinement because it is the only way to simultaneously improve the strength and toughness of steels. The grain refinement strengthening can be described by the Hall-Petch formula.

$$\sigma_g = k_y d^{-1/2} \tag{5.8}$$

where d is the effective grain size and k_y is the proportional coefficient.

Effective grain size refers to the size of the smallest grain composed of the boundaries which impede the dislocations slip and result in the pilling up of dislocations. The sub-grain boundaries cannot become the effective grains because there is generally no dislocation pilling up nearby. Ti-microalloyed steel is generally ferrite-pearlite steel and the effective grain size is the size of ferrite grains. Theoretical calculations show that the proportional coefficient k_y is about 24.7 MPa mm$^{1/2}$. A large number of experiments have confirmed the Hall-Petch formula, and the proportional coefficient k_y can be obtained according to these experimental results. The results indicate that when the strain rate is between 6×10^{-4} and 1 s^{-1} and the grain size is in the range of 3 μm to several millimeters, the proportional coefficient k_y is 14.0–23.4 MPa mm$^{1/2}$. The proportional coefficient k_y is usually set as 17.4 MPa mm$^{1/2}$ for low carbon steel.

Figure 5.26 shows the relationship between grain refinement strengthening effect and titanium content of steel sheets with the thickness of 4.00 mm. The grain refinement strengthening increment increases with the increase in the titanium content in the beginning. Then, the increment gradually reaches a stable value of about 210 MPa when the titanium content is larger than 0.045%. The grain refinement strengthening effect increases with the decrease in the thickness, as shown in Fig. 5.27.

Precipitation strengthening Precipitation strengthening increment can be obtained by subtracting the contribution of solute strengthening, grain refinement strengthening and lattice force of pure iron from the yield strength according to Eq. (5.5). Figure 5.26 shows the relationship between precipitation strengthening effect and titanium content of steel sheets with the thickness of 4.00 mm. The precipitation strengthening increment increases slowly with the increase in the titanium content initially. Then, it increases rapidly when the titanium content exceeds 0.045%, but the increase slows down when the titanium content exceeds 0.095%.

When the titanium content is less than 0.045%, titanium mainly combines with nitrogen and sulfur to form TiN and $Ti_4C_2S_2$ particles with the size ranging from several dozens to several hundred of nanometers. Among those precipitates, the smaller ones refine the grains by suppressing the growth of recrystallized austenite grains, thereby playing the role of grain refinement strengthening. In addition, they have small precipitation strengthening effect.

When the titanium content continues to increase, the excess titanium is consumed by precipitation in austenite, interphase precipitation and precipitation in

Fig. 5.26 Relationship between yield strength and titanium content of steel plates with the thickness of 4.0 mm
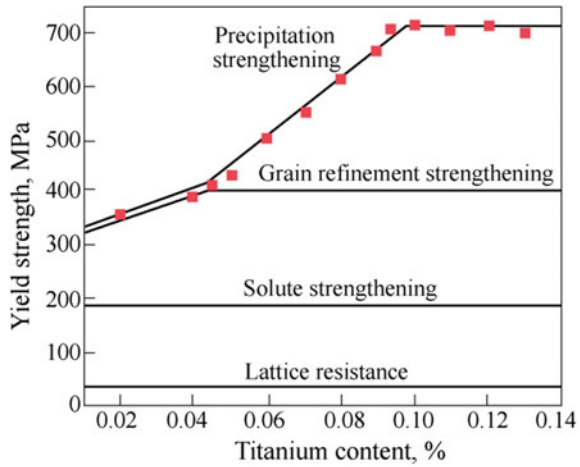
Fig. 5.27 Relationship between strengthening increment and thickness of steel strip containing 0.058% Ti
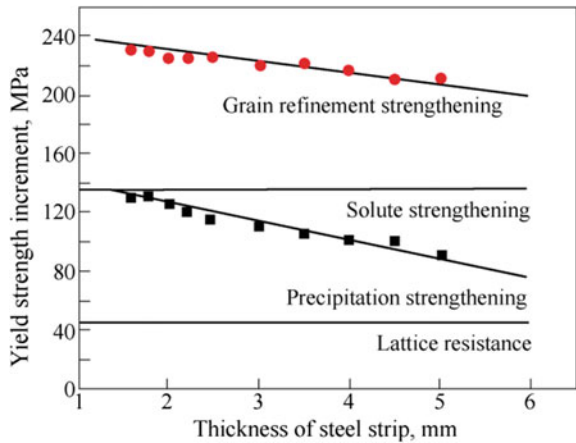
ferrite successively. These TiC precipitates are spherical and their sizes are ranging from several nanometers to several dozens of nanometers. They are massively and dispersively distributed in ferrite matrix and dislocation lines, so the precipitation strengthening effect is remarkable. In particular, the TiC particles precipitated in ferrite are the smallest because of the lowest precipitation temperature, so their precipitation strengthening effect is the strongest. Therefore, the yield strength is significantly enhanced with the increase in the titanium content when the titanium content exceeds 0.045%. The amount of TiC precipitated in ferrite is limited because the carbon content of ferrite is low. When the titanium content increases to a certain value, the carbon in ferrite completely combines with titanium to form TiC and the strengthening effect tends to saturate. When the titanium content further increases, the further strengthening effect comes from TiC particles precipitated in austenite and inter-phase precipitation. However, TiC particles tend to grow and coarsen because
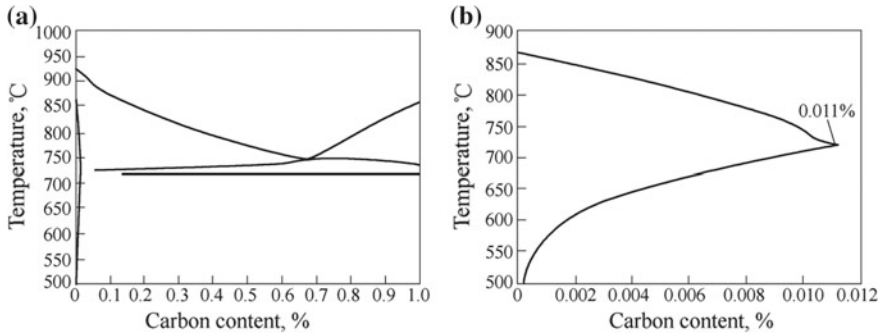
Fig. 5.28 **a** Fe (Mn, Cr, Si, P, S, Cu, P)–C phase diagram, and **b** enlarged diagram of single phase region of ferrite

the precipitation temperature is high due to the high titanium content. Therefore, their strengthening effect is not as significant as those precipitated in ferrite. The strengthening increment slows down when the titanium content exceeds 0.095%.

The maximum solubility of carbon in ferrite is 0.0218% at the eutectoid temperature according to the Fe-C binary phase diagram. The addition of alloying elements usually decreases the carbon solubility of ferrite. Figure 5.28a shows the phase diagram of Fe (Mn, Cr, Si, P, S, Cu, P)–C system of Ti-microalloyed high strength steel. Figure 5.28b is the amplification of the single phase region of ferrite, indicating the maximum solubility of carbon in ferrite is 0.011%. However, the maximum solubility of carbon in ferrite is slightly larger under the actual non-equilibrium cooling conditions. In addition, the carbon content of ferrite should be lower than the actual maximum solubility. Therefore, it can be roughly estimated that the carbon content of ferrite is 0.01%, and the carbon can combine with 0.04% titanium to form TiC. If the titanium consumptions including combination with nitrogen and sulfur, precipitation in austenite and inter-phase precipitation are taken into account, the value of the inflection point reflecting the slowdown of the strengthening increment, i.e. the second inflection point, should be no less than 0.085% Ti, which is almost consistent with the production data (0.095%).

In addition, the decrease in the steel product thickness enhances the precipitation strengthening if the titanium content is constant, as shown in Fig. 5.27. This is because when the thickness decreases, the cooling rate increases, thereby refining Ti(C, N) precipitates.

Titanium combines with carbon to form TiC in Ti-microalloyed high strength steel. TiC particles precipitated during the cooling and coiling processes are very fine and their sizes reach the magnitude of 10 nm, resulting in a significant precipitation strengthening effect. According to Gladman's theory, the precipitation strengthening effect can be quantitatively calculated.

According to the analysis above, the strengthening components of thin gauge high strength steel are estimated, as shown in Fig. 5.26 [12]. The maximum contribution of precipitation strengthening is about 250 MPa. The cooling rates of steel strips

with different thicknesses are different. As a result, the sizes and mass fractions of precipitate particles are different, so the precipitation strengthening effects are different.

Figure 5.24 shows that there are two inflection points at 0.045% and 0.095% Ti. This is because only the grain refinement strengthening and precipitation strengthening are related to the titanium content among the hardening components. When the titanium content is less than 0.045%, the yield strength increases slowly with the increase in the titanium content. There are two reasons. One is that the grain refinement strengthening effect increases the yield strength by about 20 MPa with the increase in the titanium content. The other is that the precipitation strengthening effect of TiN and $Ti_4C_2S_2$ particles is small because these particles precipitate at high temperatures and they are large (about several dozens of nanometers to several hundred of nanometers). When the titanium content is above 0.045%, the grains are no longer refined with the increase in the titanium content. The increase in the strength is mainly due to the precipitation strengthening effect of TiC precipitates. The strength increases rapidly with the titanium content because the strengthening effect from the dispersive and fine TiC particles is large. The yield strength does not increase anymore when the titanium content is higher than 0.095%, because higher titanium content leads to precipitation of TiC in austenite before rolling, and the mass fraction of TiC particles from strain induced precipitation and precipitation in ferrite remains almost unchanged.

References

1. Qu Y. Principles of steelmaking [M]. Beijing: Metallurgical Industry Press, 1994.
2. Zhu W J, Ou T, Li G Q. Influence of LF refining on T[O] and inclusions of container steel [J]. Journal of University of Science and Technology Beijing, 2011, 33(S1), 137–140.
3. Pillild C F. Variables affecting the nitrogen content of carbon and low alloy acid electric arc furnace steel [C]. Electric Furnace Conference Proceedings, ISSI, 1988, 46, 107–110.
4. Thomas J, Scheid C, Geiger G. Nitrogen control during EAF steelmaking [J]. April 1993-January 1994, I & SM.
5. Mao X P, Lin Z Y, Li L J, et al. A method of improving and stabilizing the yield of titanium of titanium microalloyed high strength weathering steel during the smelting and continuous casting process [P]. Patent: 200510102239.0, China.
6. Mao X P. Microalloying technology on thin slab casting and direct rolling process [M]. Beijing: Metallurgical Industry Press, 2008.
7. Su L, Tian N Y, Mao X P, et al. Influence of liquid core reduction on the microstructure and mechanical properties of high strength weathering steel [C]. Society of Technical Exchange and Development of Thin Slab Casting and Direct Rolling. Proceedings of the Fourth Technical Exchange Conference on Thin Slab Casting and Direct Rolling, Ma Anshan, China, 2006: 538–543.
8. Huo X D, Mao X P, Li L J, et al. Strengthening mechanism of Ti micro-alloyed high strength steels produced by thin slab casting and rolling [J]. Iron and Steel Supplement, 2005, 40: 464–468.
9. Mao X P, SunX J, WangS Z. Control rolling technology of Ti-microalloyed strip produced by TSCR [J]. Iron & Steel, 2016, 51(1): 1–7.

10. Yong Q L, Ma M T, Wu B R. Physical and mechanical metallurgy of microalloyed steel [M]. Beijing: Machinery Industry Press, 1989.
11. Yu H. Research on the microstructure refinement and strengthening mechanism of hot strip of low carbon steel produced by compact strip production [D]. Beijing: University of Science and Technology Beijing, 2003.
12. Mao X P, SunX J, Kang Y L, et al. Physical metallurgy for the titanium microalloyed strip produced by thin slab casting and rolling process [J]. Acta Metallurgica Sinica, 2006, 42(10): 1091–1095.